frontiers | Frontiers in Physics

ORIGINAL RESEARCH
published: 27 May 2022
doi: 10.3389/fphy.2022.912229

Detecting Boosting Weak Signal *via* A Meminductive Multistable Chaotic System

Baolin Kang[1] *and Wenjie Qin*[2]*

[1]School of Mathematics and Information Sciences, Anshan Normal University, Anshan, China, [2]School of Mathematics and Computer Science, Yunnan Minzu University, Kunming, China

In this paper, we rebuild a new meminductive chaotic circuit model based on a Wien-bridge oscillator. Due to the extreme multistability of the meminductive system, it can produce the phenomenon of many infinitely coexisting attractors. Systems that spontaneously produce coexisting oscillations are relatively rare in the study of meminductive circuit systems and are well suited as pseudo-random number generators (PRNG). In this study, a new weak signal detection model is established based on the proposed meminductive system. This detection model can detect boosting weak signals with different amplitudes. The trajectory of objects can be predicted effectively by the boosting line spectrum in the frequency domain. The experimental result shows the feasibility through which the meminductive multistable system is applied in the detection field.

OPEN ACCESS

Edited by:
Jun Mou,
Dalian Polytechnic University, China

Reviewed by:
Ning Wang,
Changzhou University, China
Li Xiong,
Hexi University, China

***Correspondence:**
Wenjie Qin
wenjieqin@hotmail.com

Specialty section:
This article was submitted to Interdisciplinary Physics, a section of the journal Frontiers in Physics

Received: *04 April 2022*
Accepted: *20 April 2022*
Published: *27 May 2022*

Citation:
Kang B and Qin W (2022) Detecting Boosting Weak Signal via A Meminductive Multistable Chaotic System. Front. Phys. 10:912229. doi: 10.3389/fphy.2022.912229

Keywords: chaos, extremely multistability, weak signal detection, meminductor, equivalent circuit

1 INTRODUCTION

Memristor, a nonlinear memory resistor, has been used extensively in recent studies. The concept of memristor first appeared in a paper by Chua [1]. Based on the relationship between electrical physical quantities, Chua outlines that there must be a set of relationships between the charge and the flux. In subsequent studies, Chua's team defined the resistance-like relationship between them as memristor. Until 2008, according to the conceptual model of memristor, HP laboratory manufactured the first nanoscale memristor using TiO2 material [2]. It also confirms the correctness of Chua's prediction. After further scientific certification, some researchers found that the volt-ampere characteristic curve of the memristor is a hysteresis loop due to its nonlinear characteristic [3–8]. Unlike normal volatile resistors, memristors are efficient at retaining energy, i.e. memristor is a component with a memory function. The memory properties of the memristor are a good match for the resistive components that will be used to build future artificial brains, for which it made headlines in scientific journals [9, 10]. Then, the Ventra team proposed the concept of meminductor [11], which adds better memory features to conventional storage devices.

Research on memristive circuit systems has made great progress, with continuous breakthroughs in memristive hardware [12–15]. The memristor oscillation circuit based on Chua's circuit model has become a hotspot of nonlinear system research. Due to the more nonlinear parts of the memristor, it can often produce complex dynamic behavior and higher sequence complexity. Thus, the memristive dynamical system is widely used in the related fields of physics [16–19], computer science [20–24], and cryptography [25–28]. Ye et al constructed a memristive circuit model based on Wen's bridge oscillating circuit. By replacing a memristor of the original 4D Wen's bridge oscillator, the new circuit equations with a memristor have more nonlinear terms. Based on this, the dynamic behavior of the

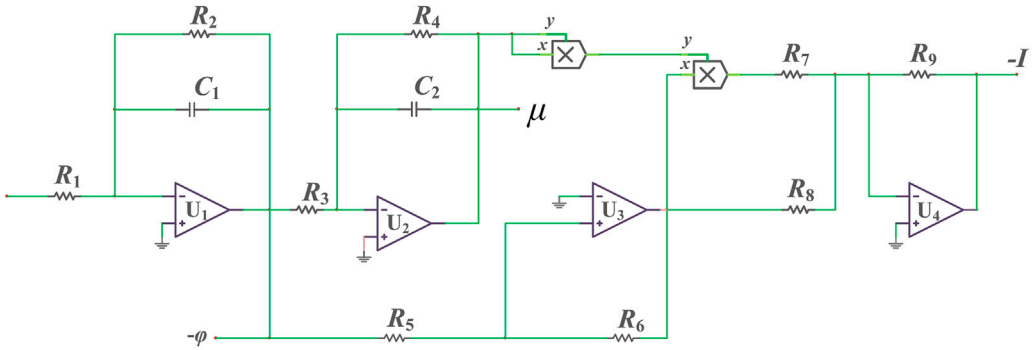

FIGURE 1 | The equivalent circuit of meminductor.

memristive circuit system becomes more complex, and there is even multi-attractor coexistence. There is even a phenomenon of multi-attractor coexistence [29]. Bao et al proposed an inductor-free memristive circuit using linear coupling of a BPF and found many coexisting infinite attractors by using numerical simulation [30]. There is a large amount of research on memristors in the existing literature. However, there are relatively few studies on meminductor, especially on the meminductive multi-stable system. Thus, it is very important to further explore complex dynamic behavior and the application of a memory-sensing system.

In this article, we focus on a novel meminductive chaotic system of extremely multistability and its application in signal detection. The article is organized as follows: in **section 2**, the meminductive equivalent circuit model is proposed. In **section 3**, the meminductive chaotic system model is built. In **section 4**, the proposed meminductive system is applied to weak signal detection. Finally, the chaotic attractors of the meminductive system are implemented by circuit experiment.

2 DESIGN OF MEMINDUCTIVE EQUIVALENT CIRCUIT

Based on the i-φ characteristics of meminductor, we have

$$i(t) = M^{-1}(\mu)\phi(t). \tag{1}$$

in the formula above, $i(t)$ and $\varphi(t)$ are the current and magnetic flux flowing through the meminductor, and $M(\mu)$ reflects the inductive resistance of the meminductor. Then, we get

$$\mu = \int_{-\infty}^{t} \varphi(\tau)d\tau. \tag{2}$$

Based on **Eqs 1**, **2**, the mathematical model of meminductor can be designed as

$$q(\mu) = a_\mu \mu + b_\mu \mu^3. \tag{3}$$

in which, a_μ and b_μ are the positive real numbers, and then we have

$$i(t) = \left(a_\mu + 3b_\mu \mu^2\right)\varphi(t). \tag{4}$$

Based on the mathematical model of the meminductor above, the equivalent circuit model of the meminductor can be designed as shown in **Figure 1**. According to the relationships of all components reflected in **Figure 1**, we can achieve the i-φ characteristic of the meminductor:

$$i(t) = \left(\frac{R_9}{R_8} + \frac{R_9}{R_7}\mu^2\right)\varphi(t). \tag{5}$$

According to **Eqs 4**, **5**, $a_\mu = R_9/R_8$ and $b_\mu = R_9/R_7$. Set the component parameters in **Figure 1** $R_1 = R_3 = R_4 = 200\text{k}\Omega$, $R_5 = R_6 = R_8 = R_9 = 10\text{k}\Omega$, $R_2 = 1\text{M}\Omega$, $R_7 = 3\text{k}\Omega$, and $C_1 = C_2 = 10\text{nF}$. By using the circuit simulation software, as shown in **Figure 2**, we can get the v-i hysteresis loop under different frequencies.

3 CONSTRUCTING A MEMINDUCTIVE CIRCUIT

3.1 Constructing a Meminductive Circuit Based on Wien-Bridge Oscillator

By building an *RLC* oscillation structure based on a Wien-bridge oscillator, a novel meminductive circuit model can be rebuilt. As reflected in **Figure 3**, the new meminductive circuit model has four resistors R_1~R_4, three capacitors, one operational amplifier, two diodes, and one meminductor.

3.2 Mathematical Model

Based on the circuit model reflected in **Figure 7**, we can obtain the circuit equations

$$\begin{cases} C_1\dfrac{du_1}{dt} = \dfrac{R_4u_1}{R_2R_3} - \dfrac{u_1}{R_1} - \dfrac{u_2}{R_2} - i_d \\ C_2\dfrac{du_2}{dt} = \dfrac{R_4u_1}{R_2R_3} - \dfrac{u_2}{R_2} \\ C_3\dfrac{du_3}{dt} = i_d - L^{-1}(\rho)\varphi \\ \dfrac{d\rho}{dt} = \varphi \\ \dfrac{d\varphi}{dt} = u_3 \end{cases}, \tag{6}$$

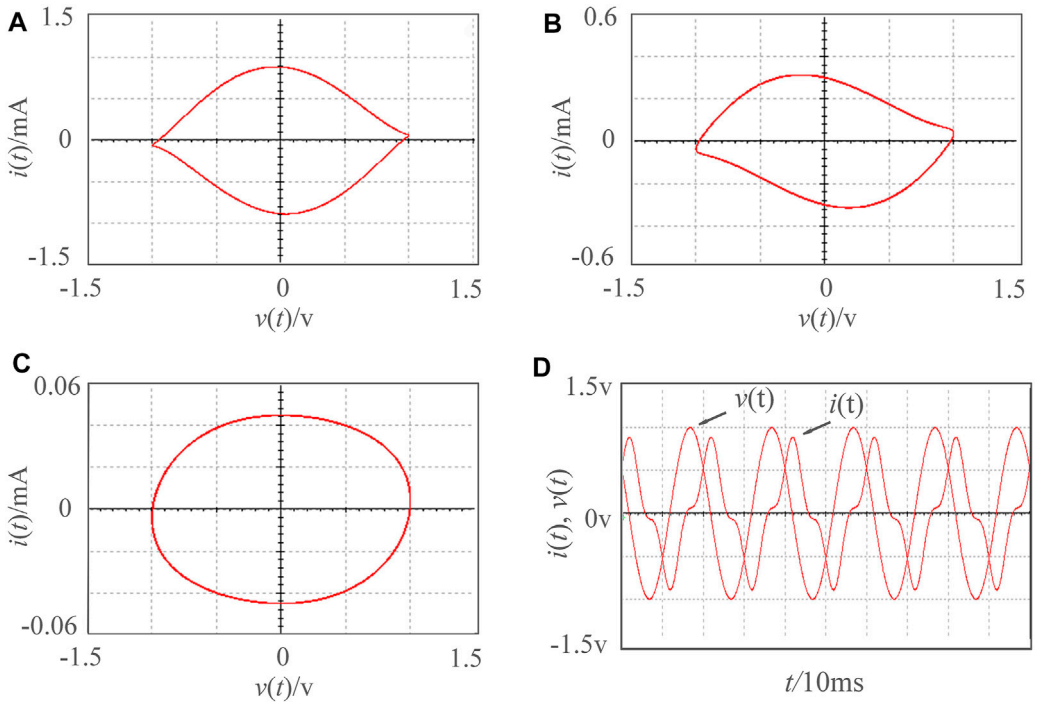

FIGURE 2 | The *v-i* hysteresis loop of a meminductive equivalent circuit under different frequencies. **(A)** *f* = 50 Hz. **(B)** *f* = 70 Hz. **(C)** *f* = 180 Hz. **(D)** waveform of *f* = 50 Hz.

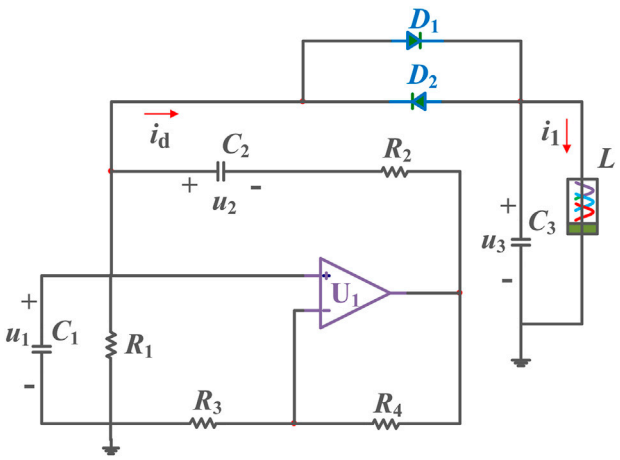

FIGURE 3 | A novel meminductive circuit based on a Wien-bridge oscillator.

in **Eq. 6**, the equations of the diodes can be expressed as

$$i_e = g_e[u_1 - u_3 + 0.5(|u_1 - u_3 - U_e| - |u_1 - u_3 + U_e|)], \quad (7)$$

in which, U_e shows the threshold voltage, g_e is the conductance. Then, let $u_1 = U_e x$, $u_2 = U_e y$, $u_3 = U_e z$, $\varphi = U_e C_1 (R_2 R_3)^{1/2} v$, $\rho = U_{th} C_1^2 R_1 R_2 w$, $i_e = U_e g_e H$, $t = C_1 (R_1 R_2)^{1/2} \tau$, $c = (R_1/R_2)^{1/2}$, $d = R_4/R_3$, $e = (R_1 R_2)^{1/2} g_e$, $C_1 = C_2 = C_3$, $a = U_e C_1 R_1 R_2 a_1$, $b = U_e^3 C_1^5 R_1^3 R_2^3 b_1$, $L^{-1}(\rho) = a + 3b\rho^2$, we have

$$H = x - z + 0.5(|x - z - 1| - |x - z + 1|). \quad (8)$$

Finally, we can get an equivalent mathematical model

$$\begin{cases} \dot{x} = (cd - 1/c)x - cy - eH \\ \dot{y} = cdx - cy \\ \dot{z} = eH - (a + 3bw^2)v \\ \dot{w} = v \\ \dot{v} = z \end{cases}. \quad (9)$$

According to the mathematical equations of the system (9), the dynamical behavior of the proposed system can be analyzed. When the system parameters are $a = 40$, $b = 10$, $c = 0.6$, $d = 8$, $e = 30$, the initial condition is (1,1,1,0.1,0.01). We can calculate Lyapunov exponents are $Ly_1 = 0.4403$, $Ly_2 = 0.0127$, $Ly_3 = 0$, $Ly_4 = -0.4536$, $Ly_5 = -35.18$. This indicates the proposed system is a hyperchaotic circuit system.

4 THE APPLICATION OF THE MEMINDUCTIVE SYSTEM IN WEAK SIGNAL DETECTION

4.1 The Construction of the Detection System Model

Due to the initial value sensitivity of chaotic systems, the system model may generate resonance signals with some weak signals. The detection model of the weak signal can be built based on the system (9). In the process of signal detection, the test weak signal is often mixed with the noise signals. In particular, some noise

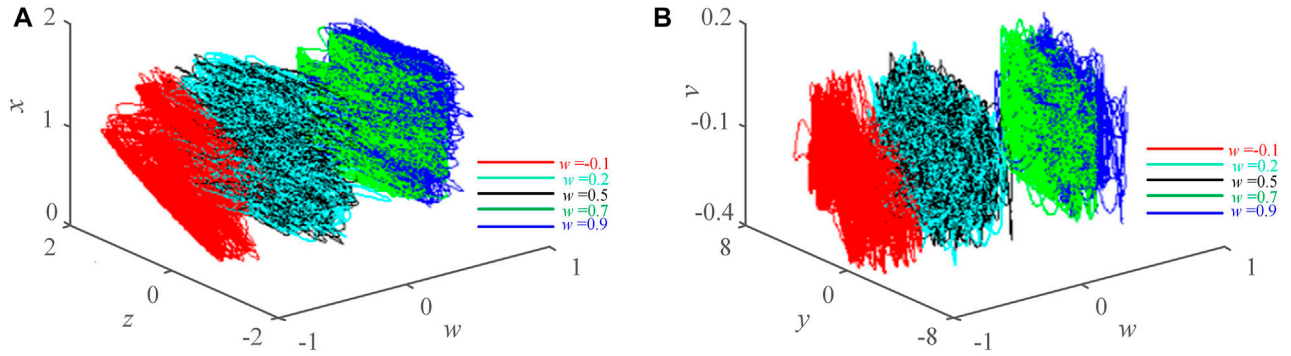

FIGURE 4 | Infinitely coexisting attractors generated by the system (10). **(A)** *x-z-w* plane. **(B)** *v-y-w* plane.

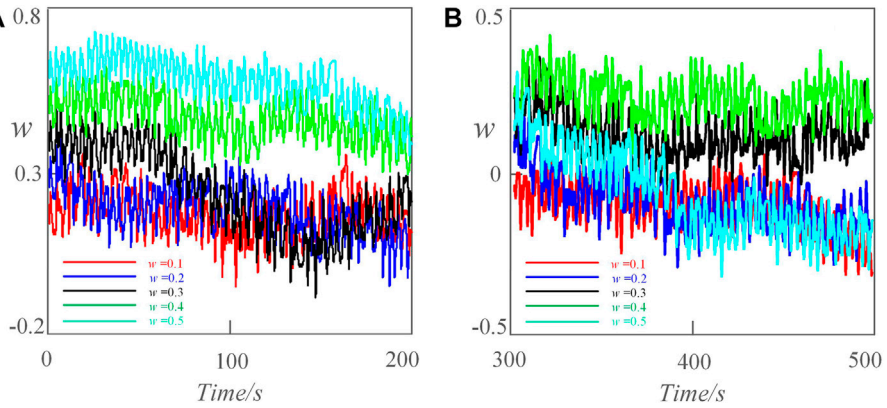

FIGURE 5 | The boosting chaos signals of the time domain. **(A)** The boost signals on *w* direction at 0–200 s. **(B)** The boost signals on *w* direction at 300–500 s.

signals have a close frequency to the test weak signal. The detection model can be expressed as

$$\begin{cases} \dot{x} = (cd - 1/c)x - cy - eH \\ \dot{y} = cdx - cy + K_1 \cos(w_1 t) + K_2 \cos(w_2 t + \varphi) \\ \dot{z} = eH - (a + 3bw^2)v \\ \dot{w} = v \\ \dot{v} = z \end{cases}, \quad (10)$$

where K_1 is the amplitude of the test weak signal, w_1 is its angular frequency. K_2 is the amplitude of the noise signal, w_2 is its angular frequency, and is its initial phase. The newly constructed detection model (10) inherits the extremely multiple stability from the meminductive system (9). Let system parameter a = 40, b = 10, c = 0.6, d = 8, e = 30, C_1 = 1, C_2 = 2, w_1 = 1, w_2 = 2, φ = 0, and the initial conditions is (1,1,1,w(0),0.01). As shown in **Figure 4**, when $w(0)$ = -0.1, 0.2, 0.5, 0.7, and 0.9 respectively, the detection model can produce infinite coexisting attractors. **Figure 5** shows the boosting signals with different amplitudes when $w(0)$ = 0.1, 0.2, 0.3, 0.4, 0.5 respectively.

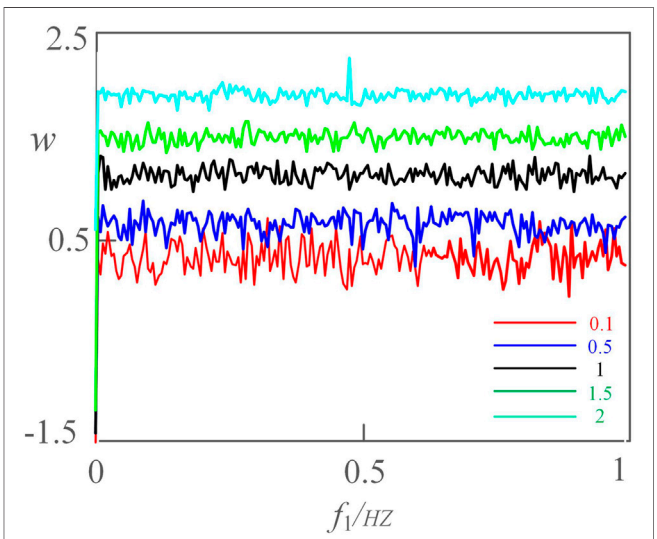

FIGURE 6 | The line spectrum of the boosting weak signal with varying amplitudes.

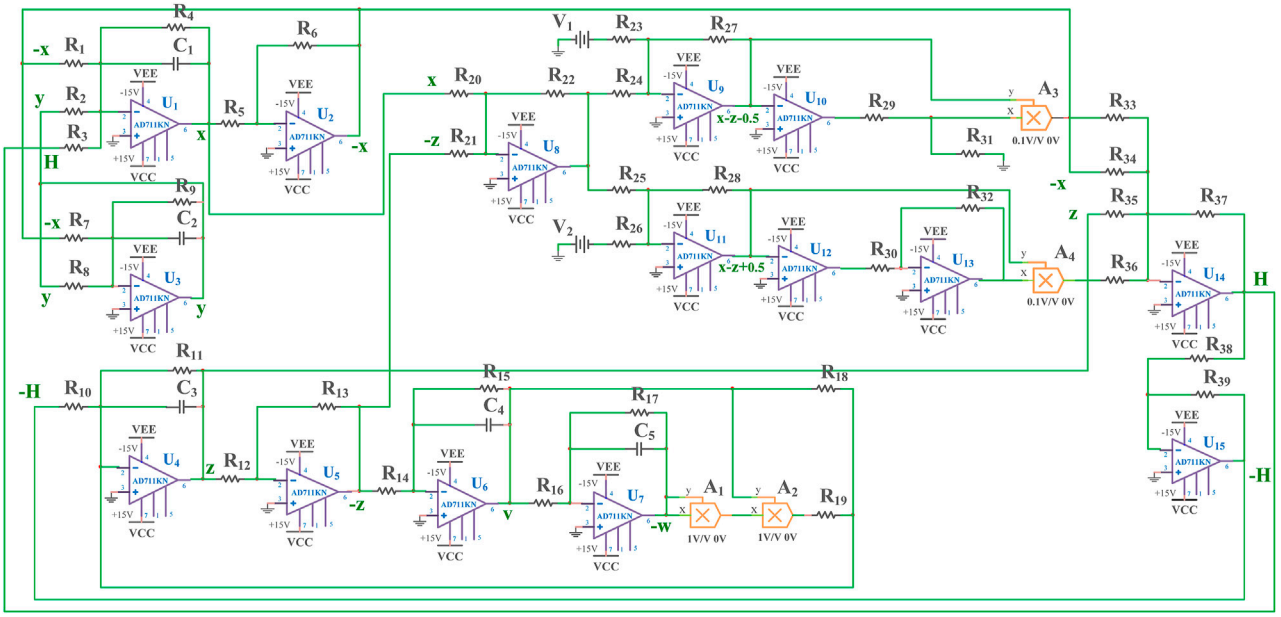

FIGURE 7 | The equivalent circuit of the proposed meminductive circuit.

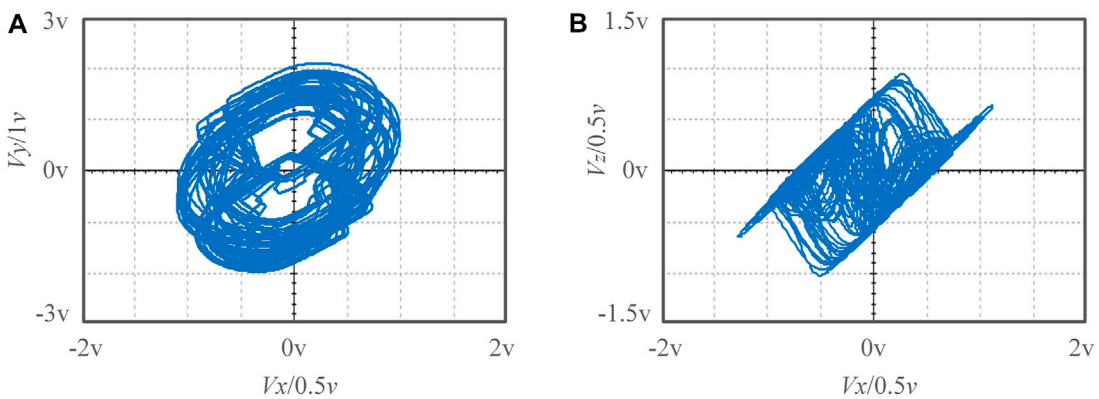

FIGURE 8 | Chaotic attractors in the circuit simulation. **(A)** V_x-V_y plane. **(B)** V_x-V_z plane.

4.2 The Extraction of the Spectral Line in the Frequency Domain

In the weak signal detection field, to understand the trajectory of the object producing the weak signal, the line spectrum in the frequency domain is often extracted. Keeping other parameters unchanged, let the initial value w = 0.1, 0.5, 1, 1.5, and 2 respectively, the line spectrum of the test signal in the frequency domain is reflected in **Figure 6**. As the initial condition w increases constantly, the corresponding amplitude of the sequence is boosting constantly, and the boosting signal can be detected within the frequency range 0–1 Hz. Due to the proposed meminductive system being extremely multistable, the useful signal can be detected within different amplitudes. Even if a detector in the amplitude range fails, the weak signals can also be detected in other amplitude ranges, which increases the fault tolerance of the detection process. These boosting signals show more useful information about the running object. Based on this key information, the trajectory of the object can be predicted.

5 REALIZATION OF THE MEMINDUCTIVE CIRCUIT SYSTEM

Doing the circuit implementation to the system (9). Based on **Eqs 8**, **9**, we have

TABLE 1 | The circuit parameters in the circuit experiment.

Resistance	Value	Resistance	Value	Resistance	Value	Others	Value
R_1	31.91 kΩ	R_{14}	100 kΩ	R_{27}	100 kΩ	C_1	100nF
R_2	166.66 kΩ	R_{15}	1 MΩ	R_{28}	100 kΩ	C_2	100nF
R_3	3.333 kΩ	R_{16}	100 kΩ	R_{29}	29 kΩ	C_3	100nF
R_4	1 MΩ	R_{17}	1 MΩ	R_{30}	129 kΩ	C_4	100nF
R_5	100 kΩ	R_{18}	2.5 kΩ	R_{31}	100 kΩ	C_5	100nF
R_6	100 kΩ	R_{19}	188.33 kΩ	R_{32}	100 kΩ	V_1	0.5 V
R_7	20.83 kΩ	R_{20}	100 kΩ	R_{33}	200 kΩ	V_2	0.5 V
R_8	166.66 kΩ	R_{21}	100 kΩ	R_{34}	100 kΩ	A_1	1
R_9	1 MΩ	R_{22}	100 kΩ	R_{35}	100 kΩ	A_2	1
R_{10}	3.333 kΩ	R_{23}	100 kΩ	R_{36}	200 kΩ	A_3	0.1
R_{11}	1 MΩ	R_{24}	100 kΩ	R_{37}	100 kΩ	A_4	0.1
R_{12}	100 kΩ	R_{25}	100 kΩ	R_{38}	100 kΩ		
R_{13}	100 kΩ	R_{26}	100 kΩ	R_{39}	100 kΩ		

$$\begin{cases} \dfrac{dX}{dT} = \dfrac{1}{R_4C_1}\left(\dfrac{R_4}{R_1}X - \dfrac{R_4}{R_2}Y - \dfrac{R_4}{R_3}H\right) \\ \dfrac{dY}{dT} = \dfrac{1}{R_9C_2}\left(\dfrac{R_9}{R_7}X - \dfrac{R_9}{R_8}Y\right) \\ \dfrac{dZ}{dT} = \dfrac{1}{R_{11}C_3}\left(-\dfrac{R_{11}}{R_{19}}W^2V - \dfrac{R_{11}}{R_{18}}V + \dfrac{R_{11}}{R_{10}}H\right), \\ \dfrac{dW}{dT} = \dfrac{R_{17}}{R_{16}C_5}V \\ \dfrac{dV}{dT} = \dfrac{R_{15}}{R_{14}C_4}Z \end{cases} \tag{11}$$

in which,

$$H = X - Z + 0.5\,(|X - Z - 1| - |X - Z + 1|). \tag{12}$$

Set $t = KT$, $x = MX$, $y = MY$, $z = MZ$, $w = MW$, $v = MV$, and set scale transformation factors $M = 2$ and $K = 100$, and we have

$$\begin{cases} \dfrac{dx}{dt} = \dfrac{1}{KR_4C_1}\left(\dfrac{R_4}{R_1}x - \dfrac{R_4}{R_2}y - \dfrac{R_4}{R_3}H'\right) \\ \dfrac{dy}{dt} = \dfrac{1}{KR_9C_2}\left(\dfrac{R_9}{R_7}x - \dfrac{R_9}{R_8}y\right) \\ \dfrac{dz}{dt} = \dfrac{1}{KR_{11}C_3}\left(-\dfrac{R_{11}}{4R_{19}}w^2v - \dfrac{R_{11}}{R_{18}}v + \dfrac{R_{11}}{R_{10}}H'\right), \\ \dfrac{dw}{dt} = \dfrac{1}{KR_{17}C_5}\dfrac{R_{17}}{R_{16}}v \\ \dfrac{dv}{dt} = \dfrac{1}{KR_{15}C_4}\dfrac{R_{15}}{R_{14}}z \end{cases} \tag{13}$$

where,

$$H' = x - z + 0.5\,(|x - z - 0.5| - |x - z + 0.5|). \tag{14}$$

In combination with the formula above, the equivalent circuit model of the system (9) can be designed as shown in **Figure 7**. Based on the equivalent circuit, as shown in **Figure 8**, the chaotic attractors can be implemented by multisim 14.0. The specific component parameters are shown in **Table 1**.

6 CONCLUSION

This proposes a new meminductive chaotic system of extreme multistability. Due to the constant shift of equilibrium with different initial values, the proposed meminductive chaotic system can generate many infinitely coexisting attractors. By introducing the model of weak signal and noise to the meminductive chaotic system, a new weak signal detection model is established. Because this detection model inherits the extreme multistability of the original meminductive system, it can detect boosting signals of different amplitudes at the same time. The spectral line in the frequency domain can effectively reflect the motion trajectory of the object generating a weak signal. Next, we will try to apply the proposed meminductive system to other related areas.

DATA AVAILABILITY STATEMENT

The original contributions presented in the study are included in the article/supplementary material, further inquiries can be directed to the corresponding authors.

AUTHOR CONTRIBUTIONS

BK: Conceptualization; Methodology; Data curation; Supervision; Investigation; Project administration; Writing—original draft; Writing—review and editing. WQ: Funding acquisition; Investigation; Project administration; Resources; Validation.

FUNDING

This work was supported by the National Natural Science Foundation of China (No: 12171004, 12026233, and 12026221).

REFERENCES

1. Chua L. Memristor-The Missing Circuit Element. *IEEE Trans Circuit Theor* (1971) 18:507–19. doi:10.1109/tct.1971.1083337
2. Tour JM, He T. The Fourth Element. *Nature* (2008) 453:42–3. doi:10.1038/453042a
3. Ma X, Li C, Wang R, Jiang Y, Leiet T. Memristive Computation-Oriented Chaos and Dynamics Control. *Front Phys* (2021) 27. doi:10.3389/fphy.2021.759913
4. Wu X, Wang H, He S. Localization of Hidden Attractors in Chua's System with Absolute Nonlinearity and its FPGA Implementation. *Front Phys* (2021) 06. doi:10.3389/fphy.2021.788329
5. Wang N, Zhang G, Kuznetsov NV, Bao H. Hidden Attractors and Multistability in a Modified Chua's Circuit. *Commun Nonlinear Sci Numer Simulation* (2021) 92:105494. doi:10.1016/j.cnsns.2020.105494
6. Wang N, Li C, Bao H, Chen M, Bao B. Generating Multi-Scroll Chua's Attractors via Simplified Piecewise-Linear Chua's Diode. *IEEE Trans Circuits Syst* (2019) 66:4767–79. doi:10.1109/tcsi.2019.2933365
7. Wang N, Zhang G, Bao H. Bursting Oscillations and Coexisting Attractors in a Simple Memristor-Capacitor-Based Chaotic Circuit. *Nonlinear Dyn* (2019) 97:1477–94. doi:10.1007/s11071-019-05067-6
8. Wang N, Zhang G, Bao H. A Simple Autonomous Chaotic Circuit with Dead-Zone Nonlinearity. *IEEE Trans Circuits Syst Express Briefs* (2020) 67:3052–6. doi:10.1109/tcsii.2020.3005726
9. Li C, Li H, Xie W, Du J. A S-type Bistable Locally Active Memristor Model and its Analog Implementation in an Oscillator Circuit. *Nonlinear Dyn* (2021) 106:1041–58. doi:10.1007/s11071-021-06814-4
10. Li C, Yang Y, Yang X, Zi X, Xiao F. A Tristable Locally Active Memristor and its Application in Hopfield Neural Network. *Nonlinear Dyn* (2022) 108:1697–717. doi:10.1007/s11071-022-07268-y
11. Di Ventra M, Pershin YV, Chua LO. Circuit Elements with Memory: Memristors, Memcapacitors, and Meminductors. *Proc IEEE* (2009) 97:1717–24. doi:10.1109/jproc.2009.2021077
12. Ma X, Mou J, Liu J, Ma C, Yang F, Zhao X. A Novel Simple Chaotic Circuit Based on Memristor-Memcapacitor. *Nonlinear Dyn* (2020) 100:2859–76. doi:10.1007/s11071-020-05601-x
13. Ye X, Wang X, Gao S, Mou J, Wang Z, Yang F. A New Chaotic Circuit with Multiple Memristors and its Application in Image Encryption. *Nonlinear Dyn* (2020) 99:1489–506. doi:10.1007/s11071-019-05370-2
14. Ye X, Mou J, Luo C, Wang Z. Dynamics Analysis of Wien-Bridge Hyperchaotic Memristive Circuit System. *Nonlinear Dyn* (2018) 92:923–33. doi:10.1007/s11071-018-4100-x
15. Xiong L, Yang F, Mou J, An X, Zhang X. A Memristive System and its Applications in Red–Blue 3D Glasses and Image Encryption Algorithm with DNA Variation. *Nonlinear Dyn* (2022) 107:1–23. doi:10.1007/s11071-021-07131-6
16. Xiong L, Zhang X, Teng S, Qi L, Zhang P. Detecting Weak Signals by Using Memristor-Involved Chua's Circuit and Verification in Experimental Platform. *Int J Bifurcation Chaos* (2020) 30:2050193. doi:10.1142/s021812742050193x
17. Ye X, Wang X. Characteristic Analysis of A Simple Fractional-Order Chaotic System with Infinitely Many Coexisting Attractors and its DSP Implementation. *Phys Scr* (2020) 95:075212. doi:10.1088/1402-4896/ab8eec
18. Liu B, Ye X, Hu G. Design of a New 3D Chaotic System Producing Infinitely Many Coexisting Attractors and its Application to Weak Signal Detection. *Int J Bifurcation Chaos* (2021) 31:2150235. doi:10.1142/s0218127421502357
19. Xu S, Wang X, Ye X. A New Fractional-Order Chaos System of Hopfield Neural Network and its Application in Image Encryption", *Chaos*A New Fractional-Order Chaos System of Hopfield Neural Network and its Application in Image Encryption. *Solitons & FractalsChaos, Solitons & Fractals* (2022) 157:111889. doi:10.1016/j.chaos.2022.111889
20. Zhou Y, Li C, Li W, Li H, Feng W, Qian K. Image Encryption Algorithm with circle index Table Scrambling and Partition Diffusion. *Nonlinear Dyn* (2021) 103:2043–61. doi:10.1007/s11071-021-06206-8
21. Li C-L, Zhou Y, Li H-M, Feng W, Du J-R. Image Encryption Scheme with Bit-Level Scrambling and Multiplication Diffusion. *Multimed Tools Appl* (2021) 80:18479–501. doi:10.1007/s11042-021-10631-7
22. Li X, Mou J, Banerjee S, Cao Y. An Optical Image Encryption Algorithm Based on Fractional-Order Laser Hyperchaotic System. *Int J Bifurcation Chaos* (2022) 32:2250035. doi:10.1142/s0218127422500353
23. Gao X, Mou J, Xiong L, Sha Y, Yan H, Cao Y. A Fast and Efficient Multiple Images Encryption Based on Single-Channel Encryption and Chaotic System. *Nonlinear Dyn* (2022) 108:613–36. doi:10.1007/s11071-021-07192-7
24. Gao X, Mou J, Banerjee S, Cao Y, Xiong L, Chen X. An Effective Multiple-Image Encryption Algorithm Based on 3D Cube and Hyperchaotic Map. *J King Saud Univ - Comp Inf Sci* (2022) 34:1535–51. doi:10.1016/j.jksuci.2022.01.017
25. Wang X, Wang X, Ma B, Li Q, Shi Y-Q. High Precision Error Prediction Algorithm Based on ridge Regression Predictor for Reversible Data Hiding. *IEEE Signal Process Lett* (2021) 28:1125–9. doi:10.1109/lsp.2021.3080181
26. Ma B, Shi YQ. A Reversible Data Hiding Scheme Based on Code Division Multiplexing. *IEEE Trans.Inform.Forensic Secur.* (2016) 11:1914–27. doi:10.1109/tifs.2016.2566261
27. Li Q, Wang X, Ma B, Wang X, Wang C, Gao S, et al. Concealed Attack for Robust Watermarking Based on Generative Model and Perceptual Loss. *IEEE Trans Circuits Syst Video Technol* (2021) 1. doi:10.1109/TCSVT.2021.3138795
28. Wang C, Ma B, Xia Z, Li J, Li Q, Shi Y-Q. Stereoscopic Image Description with Trinion Fractional-Order Continuous Orthogonal Moments. *IEEE Trans Circuits Syst Video Technol* (2022) 32:1998–2012. doi:10.1109/TCSVT.2021.3094882
29. Ye X, Wang X, Zhao H, Gao H, Zhang M. Extreme Multistability in a New Hyperchaotic Meminductive Circuit and its Circuit Implementation. *Eur Phys J Plus* (2019) 134:206. doi:10.1140/epjp/i2019-12535-0
30. Bao B, Jiang T, Xu Q, Chen M, Wu H, Hu Y. Coexisting Infinitely many Attractors in Active Band-Pass Filter-Based Memristive Circuit. *Nonlinear Dyn* (2016) 86:1711–23. doi:10.1007/s11071-016-2988-6

Conflict of Interest: The authors declare that the research was conducted in the absence of any commercial or financial relationships that could be construed as a potential conflict of interest.